Drug delivery

DOI: 10.1002/smll.200600441

Ultrasound-Triggered Release from Multilayered Capsules

*Bruno G. De Geest, Andre G. Skirtach, Arif A. Mamedov, Alexei A. Antipov, Nicholas A. Kotov, Stefaan C. De Smedt, and Gleb B. Sukhorukov**

The growing need for drug-delivery systems that release their contents in a desired fashion has intensified research for "smart carriers" with intelligent properties.[1–3] Compared to more established delivery vehicles, such as polymeric micelles,[4] liposomes, and small colloidal particles,[5] polymeric polyelectrolyte multilayered[6] capsules[7,8] are emerging materials with high potential as macromolecular drug-delivery systems.[9–12] The major advantages of these microcapsules are their loading capacity and the possibility to precisely tailor their properties by choosing the components of the capsules. Considerable amounts of macromolecular therapeutics can be encapsulated inside these capsules[13] and, depending on the choice of coating material (i.e., synthetic or biological), one can render capsules nondegradable or degradable.[11] Also, their mechanical strength can be tailored by varying the number of coating layers,[14] inclusion of nanoparticles,[15] or by thermal treatment.[16,17] Once their target site is reached, it is of utmost importance to have a mechanism that causes release of encapsulated species from these capsules. Externally triggered release has recently been shown to be possible by laser-light illumination.[18–20] The principle of this system is based on heating of metal nanoparticles, which causes changes in permeability of the outer shell and even total disruption of the shell, finally resulting in the release of the encapsulated material.[20] These laser-light-sensitive capsules could, for example, be activated after cellular uptake[21] or be used for transdermal activated-drug release.

Herein, we report the use of ultrasound to trigger release from multilayered capsules. Ultrasound has been used widely in biomedical applications[22] for improving drug uptake, anti-inflammatory treatment, or imaging. Upon propagation, an ultrasound wave undergoes both viscous and thermal absorption as well as scattering.[23,24] At low frequency the temperature difference between the particle and the medium will be in equilibrium, whereas at high frequency only a small portion of the surface will be affected by thermal waves. Similar frequency dependence is applicable to viscous losses, wherein extensive particle motion occurs at low frequency while little movement takes place at high frequencies. Figure 1 shows schematically the fabrication of the capsules and the effect of ultrasound on their integrity. When the capsules are subjected to ultrasound, a morphological change of the capsule wall occurs due to the creation of shear forces between the successive fluid layers, which results in the disruption of the capsule membrane and release of encapsulated species.

Multilayered capsules were fabricated using the LbL technique by successive coating of $CaCO_3$ microparticles with different layers of polyelectrolytes and gold nanoparticles. This process is shown schematically in Figure 1. During fabrication, the $CaCO_3$ microparticles were filled with 2000-kDa fluorescein isothiocyanate (FITC)-labeled dextran by co-precipitation. This is an elegant method, which allows a high degree of loading and avoids a post-filling step of the capsules. Co-encapsulation in $CaCO_3$ microparticles is typically performed in the case of macromolecules, and leads to a large quantity of encapsulated macromolecules without loss of biological activity.[13] This approach is less suited to the encapsulation of low-molecular-weight drugs, as such molecules would tend to diffuse outwards during LbL coating of the $CaCO_3$ microparticles, or they would diffuse outwards through the LbL membrane upon dissolution of the $CaCO_3$.

Two different types of capsules were fabricated: Type 1 consisted solely of polyelectrolytes, while type 2 were hybrid capsules consisting of polyelectrolytes and gold nanoparticles (AuNPs). Sodium poly(styrene sulfonate) (PSS) was used as polyanion while poly(allylamine hydrochloride) (PAH) was used as polycation. AuNPs were fabricated according to the method reported by Kimura et al.,[25] which resulted in AuNPs with a diameter ranging from 1 to 5 nm (as verified by transmission electron microscopy; data not shown) and a negative surface charge (as verified by measuring the electrophoretic mobility) due to the presence of carboxyl groups on the surface of the AuNPs. Multilayer buildup between the PSS/PAH (in the case of type 1 capsules) and AuNP/PAH (in the case of type 2 capsules) was driven by the electrostatic interactions between the cationic amino groups of the PAH and the anionic sulfonate of the PSS and carboxyl groups, respectively. For each type of cap-

[*] Prof. G. B. Sukhorukov
Department of Materials
Queen Mary University of London
London E1 4NS (UK)
Fax: (+44) 20-8981-9804
E-mail: g.sukhorukov@qmul.ac.uk
Dr. B. G. De Geest, Prof. S. C. De Smedt
Laboratory of General Biochemistry and Physical Pharmacy
Department of Pharmaceutics, Ghent University
Harelbekestraat 72, 9000 Ghent (Belgium)
Dr. A. G. Skirtach
Max Planck Institute of Colloids & Interfaces
Am Muehlenberg 1, 14476 Potsdam (Germany)
Dr. A. A. Mamedov
Polimaster, Inc.
2230 Clarendon Blvd., STE 708
Arlington, VA 22201 (USA)
Dr. A. A. Antipov
PlasmaChem GmbH
Rudower Chaussee 29, 12489 Berlin (Germany)
Prof. N. A. Kotov
Department of Chemical Engineering
University of Michigan
Ann Arbor, MI 48109 (USA)

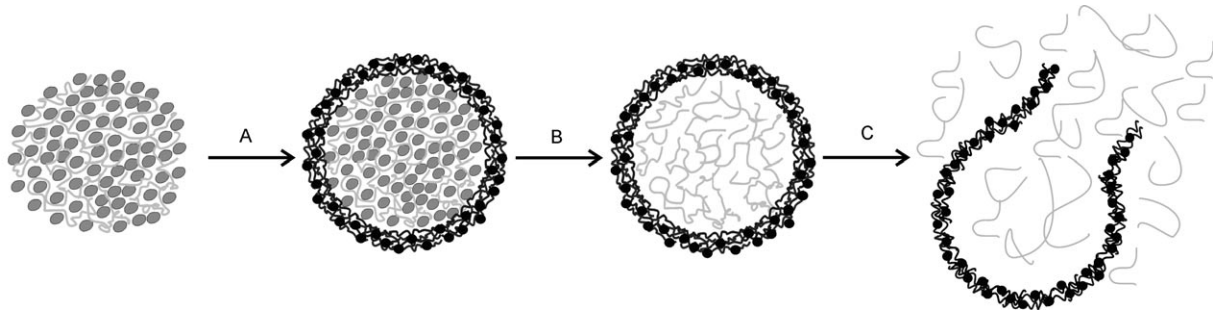

Figure 1. Schematic representation of the encapsulation and release of species in/from polyelectrolyte capsules. Calcium carbonate microparticles with macromolecules in their pores are coated with polyelectrolytes (light gray lines) and nanoparticles (black dots) using the layer-by-layer (LbL) technique (step A). After dissolution of the calcium carbonate, hollow capsules are obtained (step B). Before ultrasound irradiation, the capsules, which consist of polyelectrolytes and nanoparticles, form a closed structure that keeps high-molecular-weight species encapsulated. After ultrasound irradiation (step C) the membrane should rupture, thus leading to the release of encapsulated species.

sule a total of four bilayers was deposited on the surface of the $CaCO_3$ microparticles, followed by dissolution of the $CaCO_3$ by treatment with ethylenediaminetetraacetic acid (EDTA). EDTA forms complexes with the calcium and permeates easily through the multilayer membrane, which results in hollow capsules with an average diameter of 4 μm. The FITC-dextrans initially entrapped inside the pores of the $CaCO_3$ microparticles are too large to permeate through the multilayered membrane and stay encapsulated inside the hollow capsules.

Figure 2 shows optical transmission, confocal, and scanning electron microscopy (SEM) images of the obtained capsules. In the optical transmission images both types of capsule appear transparent. However, the $(PSS/PAH)_4$ capsules are barely visible, whereas the $(AuNP/PAH)_4$ capsules appear significantly darker. These observations are consistent with the appearance of the capsules in suspension, which is a slightly turbid but clear suspension in the case of $(PSS/PAH)_4$ capsules and a dark-brown suspension for $(AuNP/PAH)_4$ capsules. The dark appearance of the $(AuNP/PAH)_4$ capsules is due to the absorption of light by the AuNPs. In the confocal images in Figure 2B and F, a homogeneous filling of the capsules with green fluorescence is observed, which indicates no preferential accumulation of fluorescence in particular parts of the capsules. The SEM images in Figure 2C, D, G and H show in detail the morphology of the capsules. Apparently, the $(PSS/PAH)_4$ capsules have a much smoother morphology compared to the $(AuNP/PAH)_4$ capsules. This is most likely due to the presence of the AuNPs within the multilayer membrane, which offer a more rigid structure that appears rather rough upon drying.

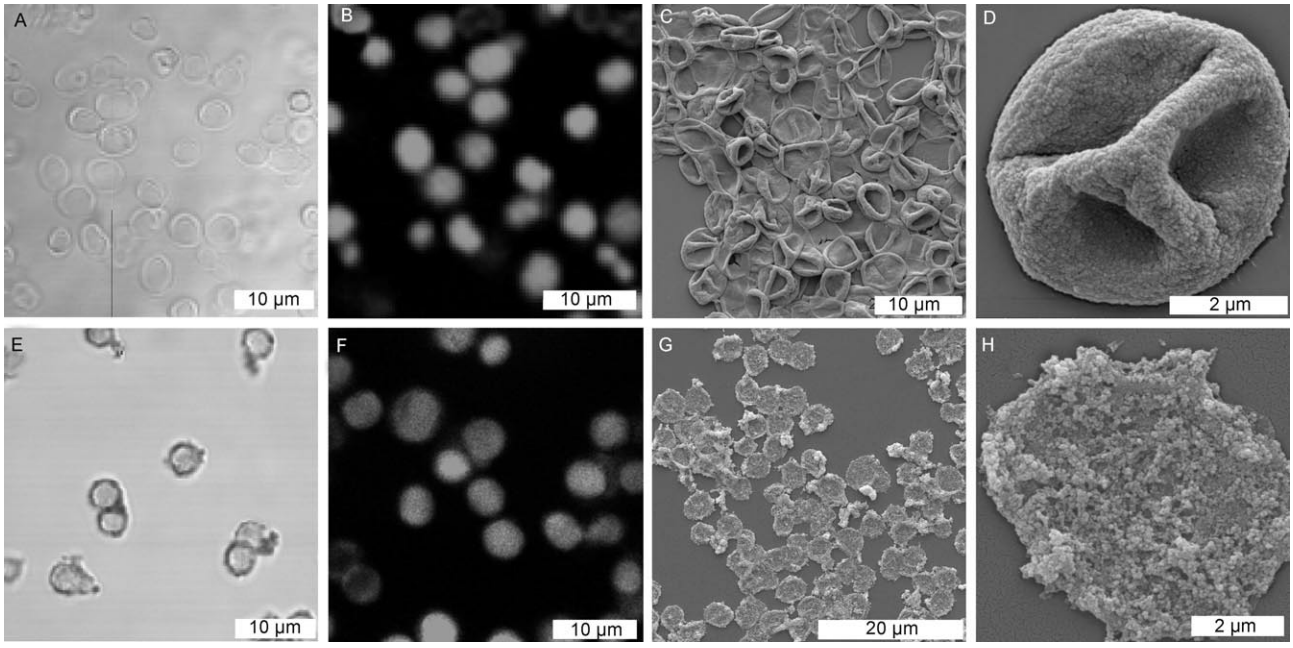

Figure 2. A, E) Optical transmission and B, F) confocal microscopy images of $(PSS/PAH)_4$ (A and B) and $(AuNP/PAH)_4$ (E and F) capsules. The contrast is due to the FITC-dextrans encapsulated in the capsules. SEM images of C, D) $(PSS/PAH)_4$ capsules and G, H) $(AuNP/PAH)_4$ capsules. Note that these images were recorded before ultrasonic treatment.

To evaluate the effect of ultrasound on the integrity of the wall of the capsules, suspensions of capsules were subjected to treatment with an ultrasonic probe operating at a frequency of 20 kHz and a power output of 20, 40, and 100 W for 1, 5, and 10 s, respectively. Initially, the capsules are nearly monodisperse spherically shaped. However, after sonication for 1 s at 20 W a large number of capsules are broken and a lot of debris of broken capsules can be detected. When the capsules are subjected to ultrasound at an output power of 100 W, almost no intact capsules are observed and nothing is left but unidentifiable debris of broken capsules. The ultrasonic shock waves originating from the ultrasound probe propagate through the liquid and cause high shear forces between the successive liquid layers. When such shear forces cleave through the membrane of the capsules, the membrane is torn apart and the capsules are destroyed. Figure 3 shows optical transmission, confocal, and SEM images of the capsules after ultrasonic treatment. The capsules are clearly destroyed and empty, the only fluorescence detected being on the walls of broken capsules due to electrostatic or hydrophobic interactions between the florescent dye and the remaining polyelectrolytes. Whereas before ultrasonic treatment the capsules had a round shape in the electron microscopy images, they are extremely deformed after ultrasonic treatment and individual capsules can hardly be detected. Figure 3 D and H shows SEM images at higher magnification of, most likely, a destroyed capsule. From the irregularities of the surface one can clearly see the impact of the ultrasound on the integrity of the capsule wall, as large holes and cracks are present.

To quantify the effect of ultrasonic treatment on the integrity of the capsules, the numbers of intact and destroyed capsules after ultrasonic treatment were determined for the different parameters of treatment time and power output. Logically, before ultrasonic treatment, no broken capsules are observed. After ultrasonic treatment for 1 s a considerable number of capsules are already broken, and increasing the treatment time results in an increasing quantity of broken capsules. Also, an increase in power input results in an increase in the number of broken capsules. These trends are presented graphically in Figure 4. Remarkably, an influence of the presence of AuNPs can also be observed. In the case when ultrasonic treatment is performed for 10 s, virtually all capsules are destroyed, irrespective of the presence of nanoparticles in the capsules' shell. However, for shorter treatment times, the capsules appear mechanically more stable when nanoparticles are included in the shell. On comparing Figure 4 A and B, one observes that after 1 and 5 s of ultrasonic treatment almost double the quantity of $(PSS/PAH)_4$ capsules are broken compared to the number of broken $(AuNP/PAH)_4$ capsules. The high density of carboxyl groups on the surface of the AuNPs[25] offers good binding sites with the PAH, which makes the multilayer structure more rigid than in the case of PSS/PAH multilayers. Therefore, such hybrid multilayers that consist of nanoparticles and polyelectrolytes are most likely more stable toward ultrasound than multilayers consisting solely of polyelectrolytes.

In conclusion, remote release of encapsulated species from multilayered capsules has been induced by ultrasound irradiation. It was shown that such irradiation has a dramatic effect on the integrity of multilayered capsules, and leads to their destruction and the release of the encapsulated species. Ultrasound offers an easy and fast way of inducing release from multilayered capsules and may be of interest to the biomedical field, for example, in topical application of ultrasound after subcutaneous injection of capsules. The capsules presented here consisted of synthetic building

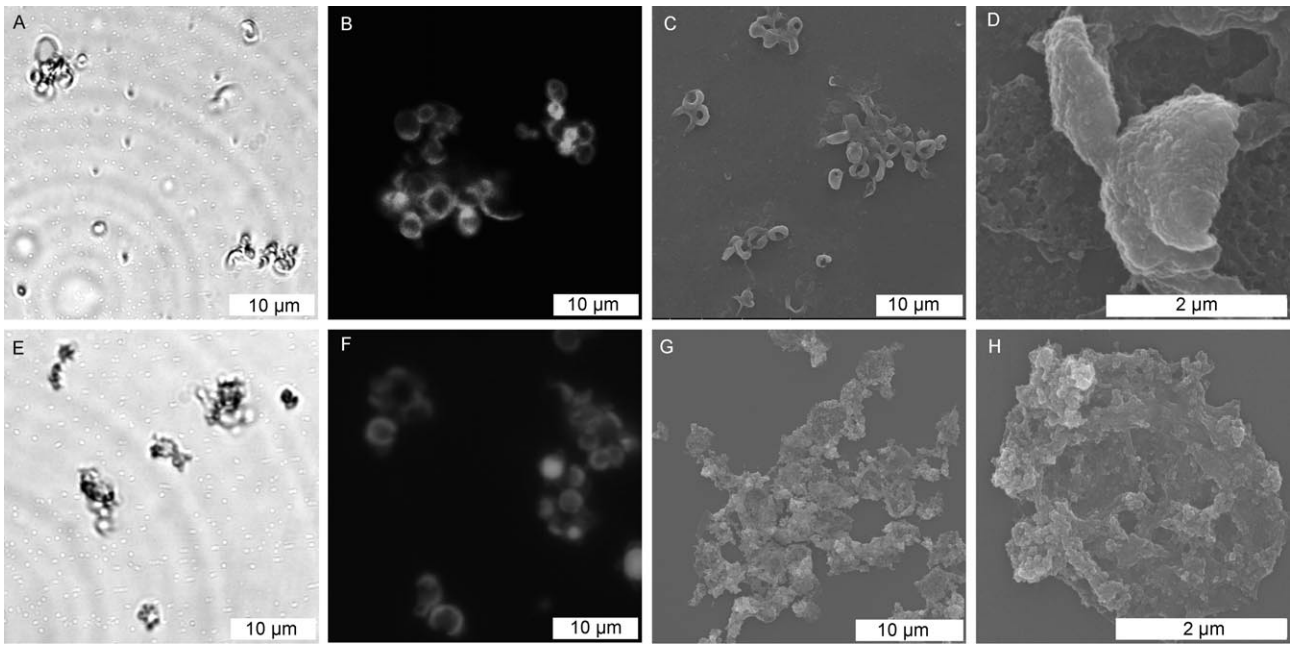

Figure 3. A, E) Optical transmission and B, F) confocal microscopy images of $(AuNP/PAH)_4$ (A and B) and $(PSS/PAH)_4$ (E and F) capsules after ultrasonic treatment. SEM images of C, D) $(PSS/PAH)_4$ capsules and G, H) $(AuNP/PAH)_4$ capsules after ultrasonic treatment.

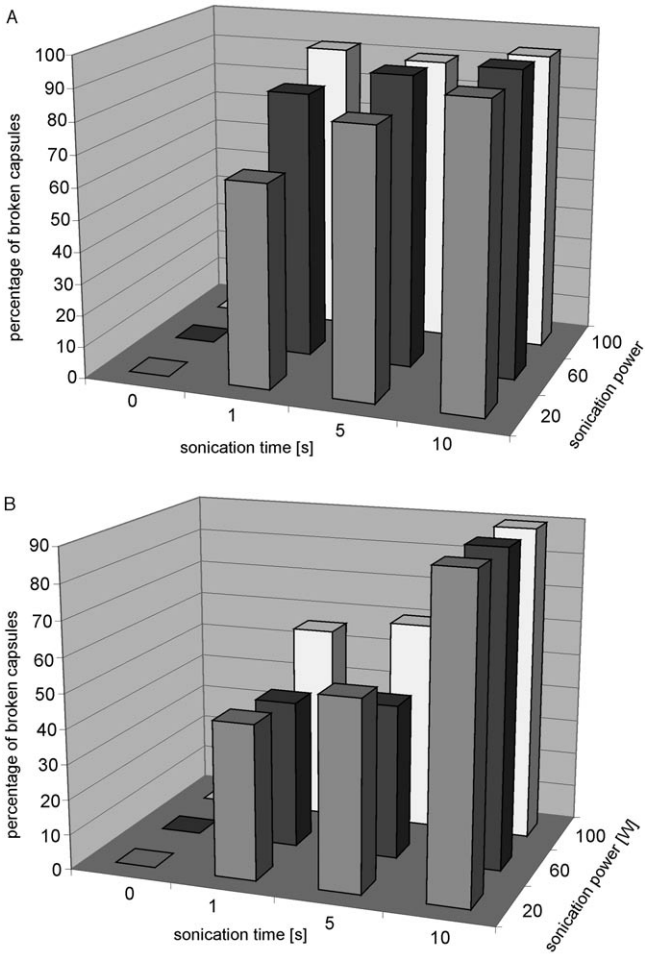

Figure 4. Percentage of broken A) $(PSS/PAH)_4$ and B) $(AuNP/PAH)_4$ capsules after ultrasound irradiation as function of irradiation time and output power. For each value 50 capsules were counted.

blocks and therefore cannot be directly translated to clinical reality, nor can the high ultrasound power that was used for the destruction of the capsules. Therefore, in our present research we are focusing on the use of biocompatible building blocks and the incorporation of ultrasound contrast agents, which could lower the required power for the breakup of capsules.

Experimental Section

Materials: PAH (weight-average molecular weight $M_w \approx 70$ kDa), PSS ($M_w \approx 70$ kDa), and FITC-dextran ($M_w \approx 2000$ kDa) were purchased from Sigma–Aldrich-Fluka. NaCl, EDTA, $CaCl_2$, and Na_2CO_3 were purchased from Merck. AuNPs were synthesized according to Kimura et al.[25] All water used in the experiments was of Milli-Q grade.

Fabrication of calcium carbonate microparticles: $CaCO_3$ microparticles were fabricated according to Volodkin et al.[26,27] Briefly, $CaCl_2$ and Na_2CO_3 solutions (0.33 M) were mixed under vigorous stirring for 30 s, which led to the precipitation of $CaCO_3$ microparticles. Subsequently, four centrifugation and washing steps with pure water were performed to remove the unreacted species. In a last step, the particles were washed with acetone and subsequently air-dried. FITC-dextran was incorporated in the $CaCO_3$ microparticles by co-precipitation.[13] Thus, FITC-dextran (5 mg) was dissolved in the $CaCl_2$ solution (3.5 mL) before mixing with the Na_2CO_3 solution.

Fabrication of multilayered capsules: Capsules were fabricated in a two-step procedure. In the first step, the $CaCO_3$ microparticles were coated using the LbL technique. FITC-dextran (20 mg) containing $CaCO_3$ microparticles was dispersed in a solution of NaCl (0.5 M) containing PSS (2 mg mL^{-1}) or AuNPs (1 mg mL^{-1}). The dispersion was continuously shaken for 10 min. The excess PSS or AuNPs were removed by two centrifugation/washing steps with deionized water. Thereafter, NaCl solution (0.5 M, 1 mL) containing PAH (2 mg mL^{-1}) was added and the dispersion was continuously shaken for 10 min, followed again by two centrifugation/washing steps. This procedure was repeated four times until four bilayers were deposited on the surface of the $CaCO_3$ microparticles. In a second step, the $CaCO_3$ core was removed by complexation with EDTA. Thus, the coated $CaCO_3$ microparticles were shaken for 30 min with EDTA solution (0.2 M, 1 mL, pH 5) followed by centrifugation and redispersion in fresh EDTA solution (1 mL). This procedure was repeated four times to ensure complete removal of the $CaCO_3$ core, as previously reported by Volodkin et al.[26] Finally, the thus obtained hollow microcapsules filled with FITC-dextran were washed four times with water.

Ultrasonic treatment: Ultrasound irradiation was performed with a Branson Sonifier 250 equipped with a titanium microtip and operated at a constant-output frequency of 20 kHz. The microtip was positioned in a suspension of capsules (250 µL) in a 500-µL Eppendorf microtube. Subsequently, ultrasound irradiation was applied at different output powers for different times.

Confocal microscopy: Confocal microscopy and transmission light microscopy images were recorded with a Biorad MRC 1024 confocal system. An inverted microscope (Eclipse TE300D, Nikon) equipped with a 60× water-immersion objective lens was used.

SEM: A drop of capsule suspension was deposited onto a silicon wafer and dried under a nitrogen stream, followed by sputtering with gold. SEM images were recorded with an FEI Quanta 200 FEG scanning electron microscope operated at an acceleration voltage of 5 kV.

Acknowledgements

Ghent University is acknowledged for a BOF scholarship. We thank Prof. Dr. H. Möhwald for support of this research. Also, the support by the 6th FP EU project STREP-NMP3-CT-2005-516922 "SelectNANO", the Volkswagen Foundation (I/80 051-054), and the 6th FP EU project STREP-001428 "NANOCAPS" are gratefully acknowledged.

Keywords:

capsules · drug delivery · encapsulation · multilayers · ultrasound

[1] M. Ferrari, *Nat. Rev. Cancer* **2005**, *5*, 161.
[2] D. A. LaVan, T. McGuire, R. Langer, *Nat. Biotechnol.* **2003**, *21*, 1184.
[3] R. Langer, D. A. Tirrell, *Nature* **2004**, *428*, 487.
[4] C. Allen, D. Maysinger, A. Eisenberg, *Colloids Surf. B* **1999**, *16*, 3.
[5] S. Faraasen, J. Voros, G. Csucs, M. Textor, H. P. Merkle, E. Walter, *Pharm. Res.* **2003**, *20*, 237.
[6] G. Decher, *Science* **1997**, *277*, 1232.
[7] E. Donath, G. B. Sukhorukov, F. Caruso, S. A. Davis, H. Mohwald, *Angew. Chem.* **1998**, *110*, 2323; *Angew. Chem. Int. Ed.* **1998**, *37*, 2202.
[8] A. A. Antipov, G. B. Sukhorukov, *Adv. Colloid Interface Sci.* **2004**, *111*, 49.
[9] H. Ai, S. A. Jones, M. M. de Villiers, Y. M. Lvov, *J. Controlled Release* **2003**, *86*, 59.
[10] B. G. De Geest, C. Dejugnat, G. B. Sukhorukov, K. Braeckmans, S. C. De Smedt, J. Demeester, *Adv. Mater.* **2005**, *17*, 2357.
[11] B. G. De Geest, R. E. Vandenbroucke, A. M. Guenther, G. B. Sukhorukov, W. E. Hennink, N. N. Sanders, J. Demeester, S. C. De Smedt, *Adv. Mater.* **2006**, *18*, 1005.
[12] B. G. De Geest, N. N. Sanders, G. B. Sukhorukov, J. Demeester, S. C. De Smedt, *Chem. Soc. Rev.*, DOI: 10.1039/b600460c.
[13] A. I. Petrov, D. V. Volodkin, G. B. Sukhorukov, *Biotechnol. Prog.* **2005**, *21*, 918.
[14] G. Ibarz, L. Dahne, E. Donath, H. Mohwald, *Macromol. Rapid Commun.* **2002**, *23*, 474.
[15] F. Dubreuil, D. G. Shchukin, G. B. Sukhorukov, A. Fery, *Macromol. Rapid Commun.* **2004**, *25*, 1078.
[16] K. Kohler, D. G. Shchukin, H. Mohwald, G. B. Sukhorukov, *J. Phys. Chem. B* **2005**, *109*, 18250.
[17] K. Kohler, D. G. Shchukin, G. B. Sukhorukov, H. Mohwald, *Macromolecules* **2004**, *37*, 9546.
[18] A. S. Angelatos, B. Radt, F. Caruso, *J. Phys. Chem. B* **2005**, *109*, 3071.
[19] B. Radt, T. A. Smith, F. Caruso, *Adv. Mater.* **2004**, *16*, 2184.
[20] A. G. Skirtach, C. Dejugnat, D. Braun, A. S. Susha, A. L. Rogach, W. J. Parak, H. Mohwald, G. B. Sukhorukov, *Nano Lett.* **2005**, *5*, 1371.
[21] A. G. Skirtach, A. Munoz Javier, O. Kreft, K. Köhler, A. Alberola Piera, H. Mohwald, W. J. Parak, G. B. Sukhorukov, *Angew. Chem.* **2006**, *118*, 4728; *Angew. Chem. Int. Ed.* **2006**, *45*, 4612.
[22] M. R. Prausnitz, S. Mitragotri, R. Langer, *Nat. Rev. Drug Discovery* **2004**, *3*, 115.
[23] J. Busby, E. G. Richardson, *Proc. Phys. Soc. London Sect. B* **1956**, *69*, 193.
[24] C. L. Morfey, *J. Sound Vibration* **1968**, *8*, 156.
[25] S. H. Chen, K. Kimura, *Langmuir* **1999**, *15*, 1075.
[26] D. V. Volodkin, A. I. Petrov, M. Prevot, G. B. Sukhorukov, *Langmuir* **2004**, *20*, 3398.
[27] D. V. Volodkin, N. I. Larionova, G. B. Sukhorukov, *Biomacromolecules* **2004**, *5*, 1962.

Received: August 22, 2006
Revised: November 22, 2006
Published online on March 27, 2007

